Auxiliary Bearing Design and Rotor Drop Analysis of High Speed Motor Compressor/AMB System

Jianming Cao [a], Paul Allaire [a], Brad Nichols [a], Tim Dimond [a], Xianhao Ma [b], Raojing Shang [b], Chunyan Wang [b], Huajun Wang [b]

[a] Rotor Bearing Solutions International, LLC, 805 Emerson Drive, Charlottesville, VA 22911, USA, paul.allaire@rotorsolution.com
[b] Suzhou Palboom Electric Co., Ltd., 1/F, Building B, Fenghuang Avenue 7, 39501 Suzhou City, China

***Abstract*—This paper presents the auxiliary bearing design and rotor drop analysis of a single stage motor-compressor. The auxiliary bearing design consists of double row, ceramic ball bearings with cages and with high axial preload. The axial preload is provided by Bellville washers which also provide axial spring stiffness and damping. The auxiliary bearings are laterally mounted on tolerance ring wave springs which provide support stiffness and damping to help absorb the impacts due to the rotor drop. A nonlinear transient rotor dynamics and auxiliary bearing modeling code has been utilized to carry out the rotor drop analysis. The very large mathematical model includes all of the shaft degrees of freedom, the auxiliary bearing races and all of the balls, as well as the Bellville washers and the wave springs. The rotor orbits, the inner and outer race orbits and the ball displacements are all evaluated versus time during the drop. The orbits were found to simply oscillate in the bottom of the auxiliary bearings and do not go into large orbit whirls. Also, the auxiliary bearing maximum compressive stress levels were evaluated and found to be well below the material yield stresses indicating long auxiliary bearing life in terms of number of drops without damaging the auxiliary bearings.**

I. INTRODUCTION

AMBs have many advantages over conventional mechanical bearings. They enable the control of the rotor position and vibration levels through feedback control. However, the properly designed backup bearing system is necessary to protect the AMBs and the rotor in the event of loss of electrical power. The event can be either a short time or a long time loss of electrical power, system overload of AMB support capability, or other equipment failure. In AMB systems, the auxiliary bearings are used to protect the magnetic bearings, the rotor, and the stator, including critical machine components such as seals from damage [1].

The most common solution for the auxiliary bearings are rolling element bearings due to low friction (minimizes heat and wear), radial and thrust load capability, and minimum volume [2]. Rotor drop happens when the system suddenly loses suspension during operation and a very detailed evaluation of auxiliary bearing system during the rotor drop is needed. The understanding and mathematical modeling of auxiliary (backup) bearings has been made a priority by the American Petroleum Institute using analytical or experimental methods [3]. Some previous testing of auxiliary bearings for AMB has been described in [4-6]. One main difference between AMBs and auxiliary bearings is that auxiliary bearings are consumable protective devices that can be replaced after several drops. However, the analysis methods for handling the drop problem are nonlinear due to contact on and off during the event [7-9]. The full system modeling results in heavy computational time.

To more accurately describe rotor behavior, a full nonlinear time transient analysis of the flexible rotor with rolling element bearings has been developed. Typically rolling element static analyses are based on constant bearing rotational speed. However, in the case of auxiliary bearings, the rotating speed changes rapidly and the loads are impact loads. For modelling of rolling element bearings, the essential and advanced technology is given by Harris [10-11]. The method uses the operating speed, bearing geometry and external applied load to calculate dry Hertzian contact stiffness and damping coefficients between raceway and ball, angular contact angle, and ball behaviors have been published [12]. For rotor drop analysis, impact loading due to contact between shaft and inner race surface is the applied force to the auxiliary bearings. Furthermore, the preloaded auxiliary bearings have flexible damped supports which are applied to the auxiliary bearing system to avoid potential auxiliary damage under the first several impact loads [13]. Evaluation of the whole auxiliary bearing system makes the problem more complicated [14-18]. Heavy computer running time has to be carefully considered for the type of nonlinear solver used as well.

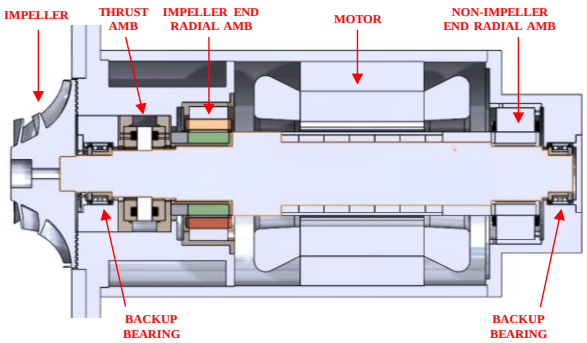

Figure 1. Schematic of High Speed Motor-Compressor Geometry.

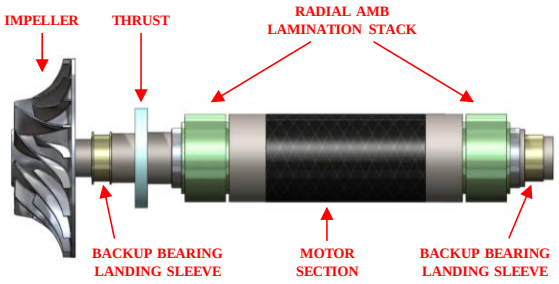

Figure 2. Schematic of High Speed Motor-Compressor Rotor.

II. Motor Compressor Configuration

The high speed motor compressor design geometry is shown in Fig. 1 and the rotor geometry is illustrated in Fig. 2.

The rotor operating speed is 20,000 rpm, the rotor total weight is 97.2 kg, and the overall length is 952 mm. The magnetic bearing system is 5 axes, 2 radial and 1 thrust. There are 2 touchdown bearings, angular contact double row ceramic ball bearing without a cage.

III. Auxiliary Bearing Design

The auxiliary bearing used in this motor-compressor unit is an angular contact ball bearing with ceramic balls and no cage. The geometry is shown in Fig. 3, obtained from Cerobear GmbH, Germany.

Figure 3. Geometry of Cerobear Angular Contract Ceramic Cageless Auxiliary Bearing.

The auxiliary bearing is a double row ball bearing with housing, axial preload with Bellville washers, landing sleeve, and wave springs as shown in Fig. 4. The bearing has axial preload to provide good angular contact between bearing races and balls so that the auxiliary bearings can withstand both radial and axial loads. The axial preload is produced by a set of Bellville washers, as illustrated in Fig 4. In this configuration, the radial gap is 0.25 mm. The axial airgap placed between the rotor and bearing outer race is 0.25 mm as well.

The Belleville washer geometry is shown in Fig. 5. The tapered Bellville washer geometry can be compressed during auxiliary bearing assembly. The axial tension can be adjusted by varying the number of washers as well as the taper angle on the washer. .

The wave spring and damping element, shown in Fig. 6, encircles the auxiliary bearings to provide both flexible

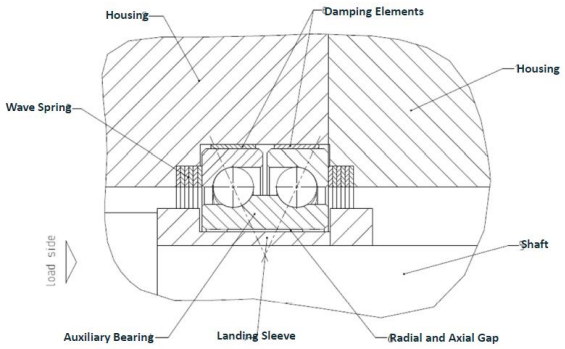

Figure 4. Auxiliary Bearing with Housing, Axial Preload with Bellville Washers, Landing Sleeve, and Wave Springs

supports for a softer landing and damping to reduce vibration amplitudes during the rotor drops. Different wave spring configurations are available from suppliers.

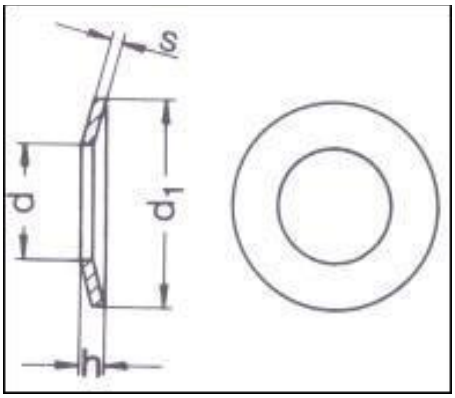

Figure 5. Bellville Washer Geometry

IV. Rotor Drop Analysis Methodology

The rotor drop analysis is carried out to evaluate the rotor orbits that arise when the power for the magnetic bearings is lost unexpectedly. The auxiliary bearings do not rotate during normal rotor operation at speed. Normally, the rotor is levitated in the magnetic bearings before the motor starts the rotor rotating. If the AMB power is lost, the rotor then drops on the auxiliary bearings. The rotor then impacts the inner race of the auxiliary ball bearings. The rotor drop analysis is a nonlinear rotor transient analysis which is carried out as a numerical modeling software program. The linear shaft model in the software is a 12 degrees of freedom (DOF) beam finite model including lateral, torsional, and axial displacements. The 12 DOF finite element is shown in Fig. 7.

Now the auxiliary bearing model is discussed. The auxiliary bearing part of the rotor drop analysis involves a Hertzian dry friction contact model along the ball/inner or ball/outer race contact areas as shown in Fig. 8. This rotor drop

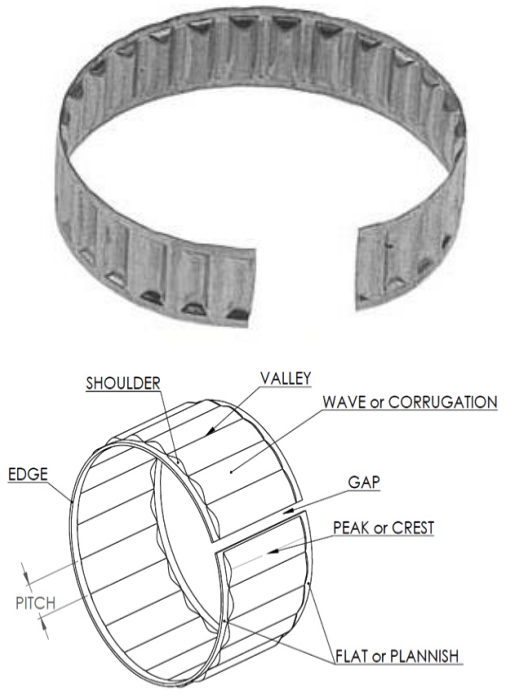

Figure 6. W
ave Spring Flexible Support and Damping Element

analysis includes all of the balls in the auxiliary bearings, as illustrated in Fig.9. The radial force acting upon the ball/inner race and ball/outer race contacts are illustrated in Fig. 9.

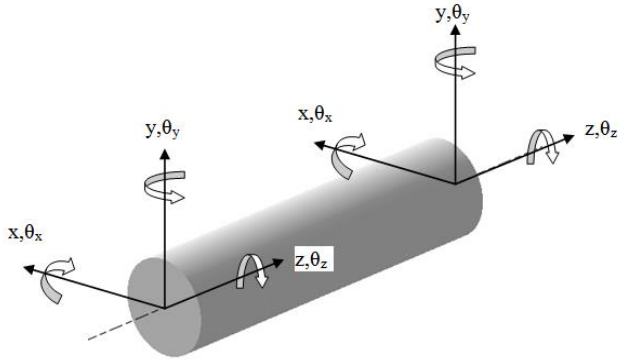

Figure 7. T
welve degree of freedom finite element beam rotor model

The initial radial and axial airgaps for the auxiliary bearings are illustrated in Fig. 10. The geometry of the balls in the auxiliary bearing is shown in Fig. 11. The balls undergo rotation in multiple directions, as illustrated in Fig. 11. The ball contact angle between the inner and outer races, is also illustrated in Fig. 11.

The impeller end auxiliary bearing takes radial and axial loads while the opposite impeller end auxiliary bearing takes the radial load only. The finite element model of the rotor also showing the auxiliary bearing locations is given in Fig. 12. The unbalance location was taken at the impeller with magnitude 112.24 g-mm, corresponding to ISO G2.5 balance grade. The original AMB closed loop stiffness was $2 \cdot 10^7$ N/m and closed loop damping was $1 \cdot 10^4$ N-s/m. The thrust load from the

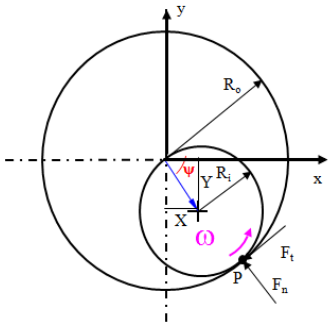

Figure 8. H
ertzian Contact Geometry in Rolling or Sliding Friction

impeller was evaluated as 1,950 N. The auxiliary bearing airgap was taken as 0.25 mm and the axial airgap as 0.25 mm.

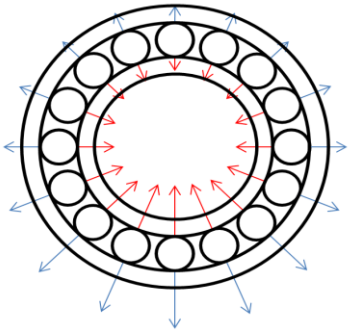

Figure 9. H
ertzian Dry Contact Between Balls/Inner Race or Balls/Outer Race Due to

V. Rotor Drop Results

The initial shaft orbits before the rotor drop are illustrated in Fig. 13 with the magnetic bearings in operation. The original AMB closed loop stiffness was $2 \cdot 10^7$ N/m and closed loop damping was $1 \cdot 10^4$ N-s/m.

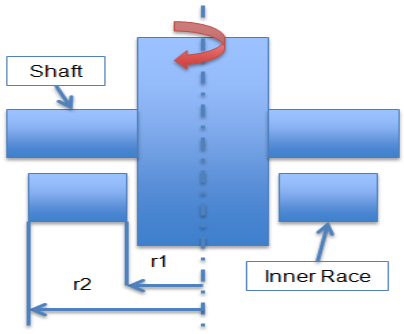

Figure 10. C
utaway View of Auxiliary Bearing and Airgap Geometry

The rotor *x* and *y* direction orbits at the auxiliary bearing 1, near the impeller, are shown in Fig. 14. This is the desired type of drop orbit which does not go into large whirl motions. The axial motion plot, both displacement and velocity versus time is given in Fig; 14, showing the rapid decay with time. The lateral orbits at auxiliary bearing 2, at the non-impeller end, are shown in Fig. 15. The orbits are similar to those at the auxiliary

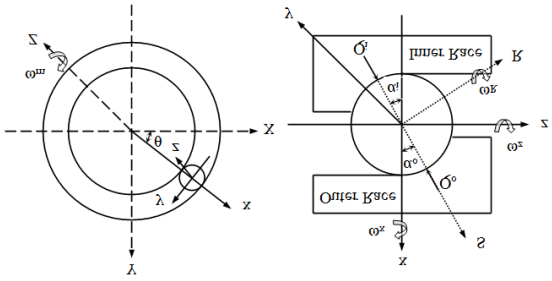

Figure 11. B
all and Race Geometry for Angular Contact Auxiliary Bearings with Contact

bearing at the non-impeller end. Again, the orbits only oscillate in the bottom of the bearing and do not go into large amplitude whirl.

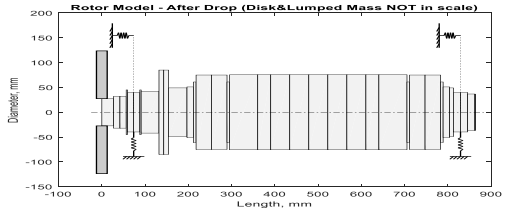

Figure 12. R
otor Finite Element Method Showing Auxiliary Bearing Locations

The unbalance location was taken at the impeller with magnitude 112.24 g-mm, corresponding to ISO G2.5 balance grade. The thrust load from the impeller was evaluated as 1,950 N. The auxiliary bearing airgap was taken as 0.25 mm and the axial airgap as 0.25 mm.

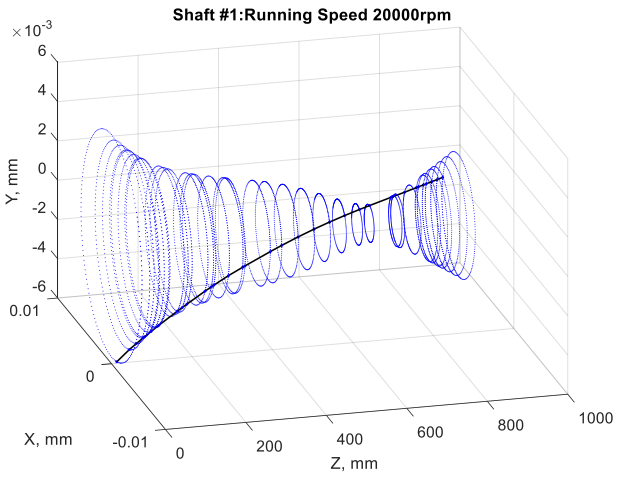

Figure 13. Initial Shaft Orbits Before Rotor Drop

These results show that the rotor drops directly to the bottom of the auxiliary bearing and then oscillates in a small amplitude, back and forth orbit near the bottom of the auxiliary bearing.

The relative motion orbit of shaft vs. inner race of auxiliary bearings 1 and 2 are shown in the upper two plots in Fig. 16. The two lower plots show the rotational speeds of the inner races in auxiliary bearings 1 and 2. It is clear that the inner race of auxiliary bearing 2 increases much more rapidly, to the

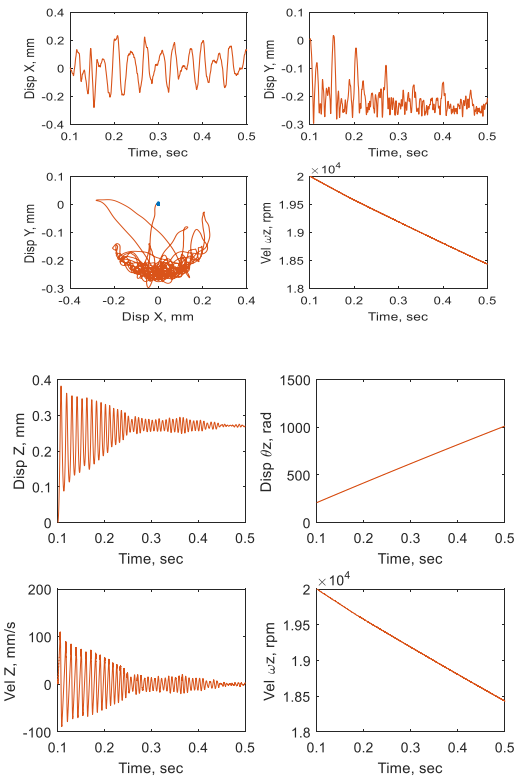

Figure 14. Rotor Lateral Orbits and Axial Vibrations at Auxiliary Bearing 1, Impeller End

operating speed of 20,000 rpm in approximately 0.1 sec following the rotor drop event. The unbalance load is taken in the impeller, due to the impeller unbalance, so the rapid acceleration of the inner race 2 prevents any major damage from occurring in the auxiliary bearings. The calculated shaft

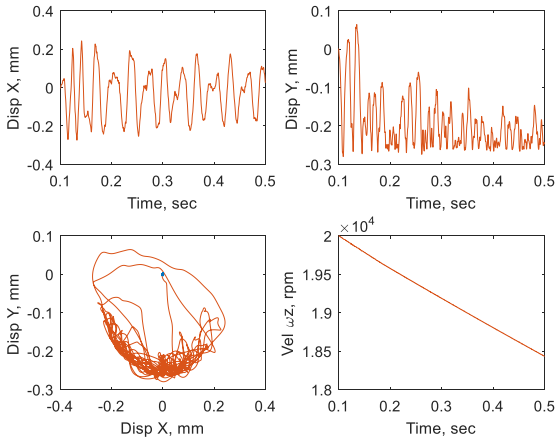

Figure 15. Rotor Lateral Orbits at Auxiliary Bearing 2, at Non-Impeller End

orbits at the time of 0.5 sec are shown in Fig. 17.

The maximum stresses in the first ball/inner race is shown in Fig. 18. The maximum stresses in the second ball/outer race in the first ball/outer race is given in Fig. 19. From these calculated values, we see that the maximum inner race stress for

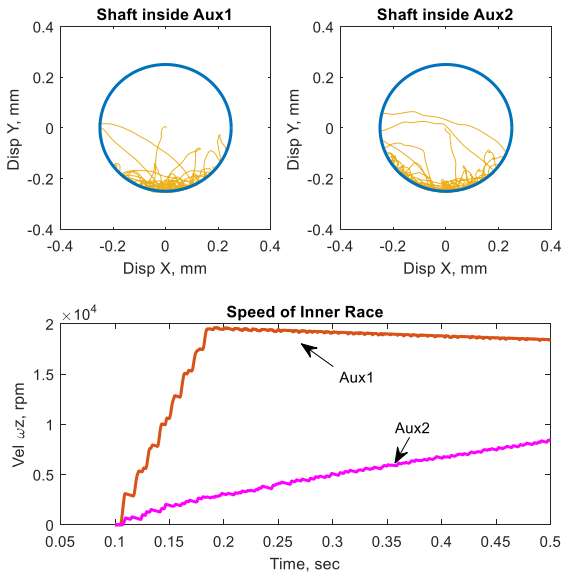

Figure 16. Upper: Shaft Orbits Inside of Auxiliary Bearings 1 and 2. Lower: Variation of Rotatioanl Speed of Inner Races of Auxiliary Bearings 1 and 2

the second row is approximately 3,200 MPa, which occurs in the first two touchdowns. The maximum outer row stress values are approximately 2,000 MPa. The maximum values for the second row are much lower.

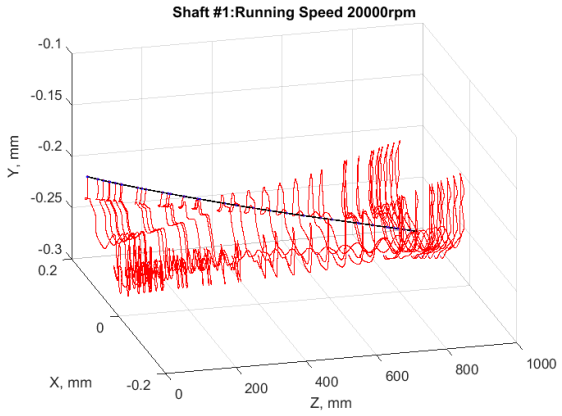

Figure 17. Shaft Orbit at 0.5 s at Operating Speed of 20,000 rpm

The contact forces on the auxiliary bearing 1 are given in Fig. 20. The radial contact forces are given in Fig. 20 with a maximum value of 6,500 N and the axial contact forces with a maximum value of 11,000 N are given in Fig. 20. We note that the contact maximum forces all occur in the first several impact touchdowns. These values yield approximate values of acceleration of 6X to 8X static radial and axial loads respectively. The contact forces on the auxiliary bearing 2 are given in Fig. 20 with the radial contact forces (upper) and axial contact forces (lower). The maximum radial contact force is 4,500 N and there is no axial contact force by design.

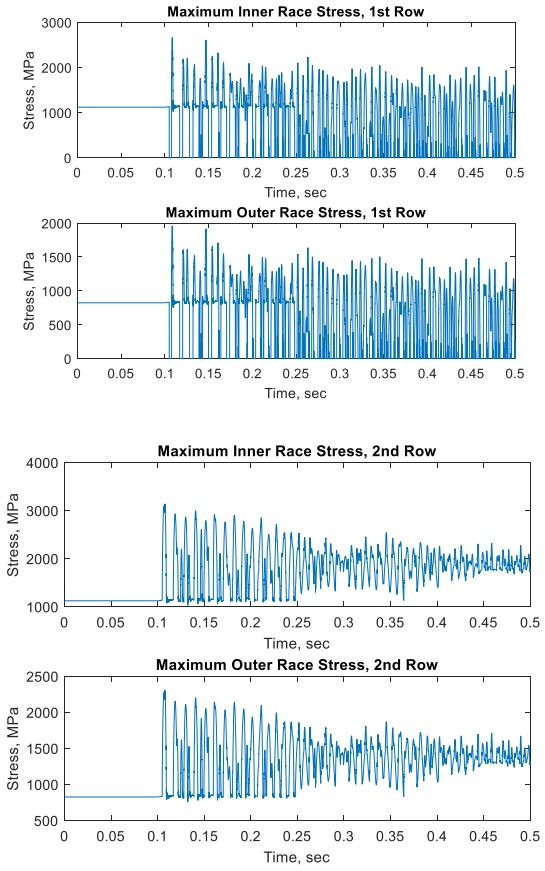

Figure 18. Maximum Inner and Outer Race Stresses in the First and Second Ball Bearing/Race Row for Auxiliary Bearing 1

VI. Conclusions

This paper presents a detailed analysis of a high speed industrial motor compressor when a power loss even happens and the rotor drops into the auxiliary bearings. The auxiliary bearings, including dual angular contact ceramic cageless ball bearings, were selected for this motor-compressor. The Bellville washers which provide axial preload on the ball bearings as well as stiffness and damping were designed for this unit. Also, wavy flexible spring supports were designed to provide lateral stiffness and damping to reduce lateral contact forces and damping to further reduce lateral vibration levels over time.

A very detailed nonlinear transient analysis was carried out to evaluate the lateral orbits and axial motions. The nonlinear analysis included the flexible rotor, the inner and outer races, all of the balls in the bearings, the Bellville washers and the wavy spring supports. The calculated lateral orbits in both auxiliary bearings 1 and 2 were found to have low amplitude back and forth orbits in the bottom of the auxiliary bearings with no large whirl orbits. Thus the auxiliary bearings provide excellent supports during the rotor impacts. In the second row of auxiliary bearing 2, the maximum inner race stress for the second row is approximately 3,200 MPa which occurs in the first two touchdowns. The maximum outer row stress values are approximately 2,000 MPa. The maximum values for the second row are much lower. Thus, these calculated values indicate that the auxiliary bearing design is very good for

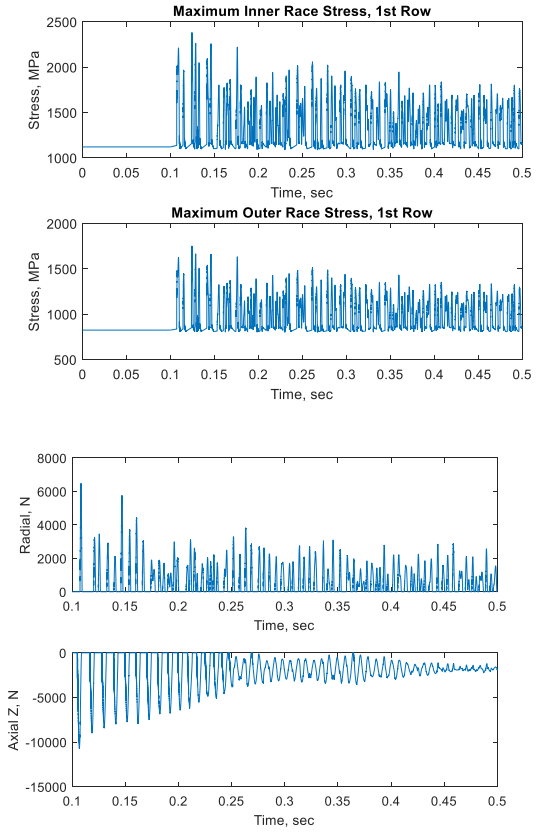

Figure 19. Maximum Inner and Outer Race Stresses in the First and Second Ball Bearing/Race Row for Auxiliary Bearing 2

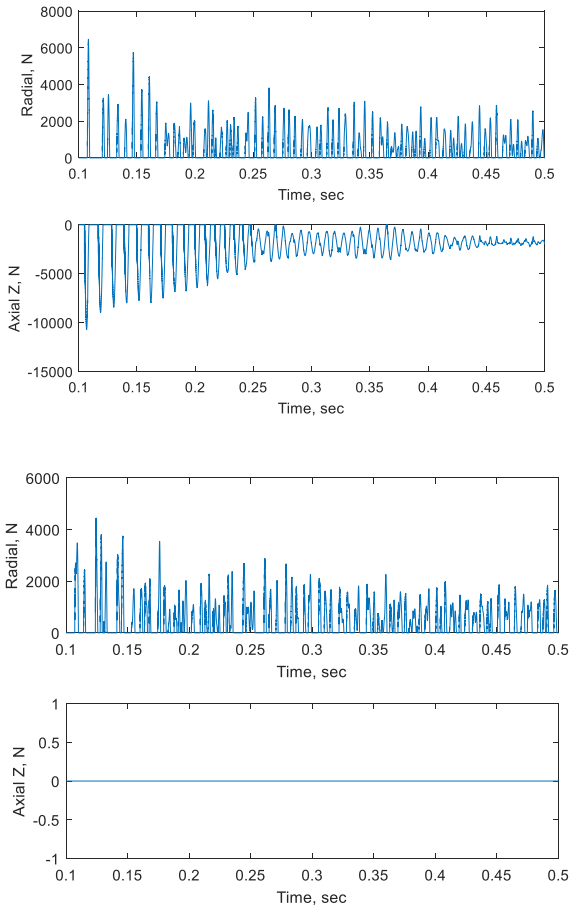

Figure 20. Contact Forces in Auxiliary Bearings 1 and 2 for Both Radial and Axial Directions

absorbing the rotor drop impacts and should be able to withstand many rotor drops without damage.

REFERENCES

[1] G. Sun, *Auxiliary Bearing Design Guides in Active Magnetic Bearing System*, VDM Verlag, Saarbrücken, Germany, 2008.

[2] Cerobear GmbH, "Auxiliary Rolling Bearing Solutions for AMB," from http://www.cerobear.com/index.php?id=248&L=1, accessed July 20, 2018

[3] API Standard 617, "Axial and Centrifugal Compressors and Expander-compressors for Petroleum, Chemical and Gas Industry Services," 8th Ed., American Petroleum Institute, Washington, D.C, 2014

[4] L. Hawkins, A. Filatov, S. Imani, and D. Prosser, 2006, "Test Results and Analytical Predictions for Rotor Drop Testing of an AMB Expander/Generator," *ASME J. Eng Gas Turbines Power*, vol. 129, no.2, pp. 522-529, 2006

[5] D. Ransom, A. Masala, J. Moore, G. Vannini, and M. Camatti, "Numerical and Experimental Simulation of a Vertical High Speed Motorcompressor Rotor Drop onto Catcher Bearings," *J. Sys. Design Dynamics*, vol. 3, no. 4, pp. 596–606, 2009

[6] J. Rensburg, "Delevitation Modelling of an Active Magnetic Bearing Supported Rotor," PhD Thesis, North-West University, Potchefstroom, South Africa, 2014

[7] A. Younan, J. Cao, T. Dimond, and P. E. Allaire, "Nonlinear Analysis of Squeeze Film Damper with Entrained Air in Rotordynamic Systems," *STLE Tribology Transactions*, vol 54, no. 1, pp. 132-144, 2010.

[8] J. Cao, T. Dimond, A. Younan, and P. Allaire, "Nonlinear Modeling of Tilting-Pad Bearing with Application to a Flexible Rotor Analysis," Proceedings of the ASME 2013 International Design Engineering Technical Conferences: 22nd Reliability, Stress Analysis, and Failure Prevention Conference; 25th Conference on Mechanical Vibration and Noise, vol. 8, DETC2013-13712, 2013.

[9] J. Cao, T. W. Dimond, and P. E. Allaire, 2015, "Coupled Lateral and Torsional Nonlinear Transient Rotor-Bearing System Analysis with Applications," *ASME J. Dyn. Sys., Meas., Control*, vol. 137, no. 9, (9): 091011, 9 pp., 2015.

[10] T. A. Harris, and M. N. Kotzalas, 2007, *Rolling Bearing Analysis: Essential Concepts of Bearing Technology*, 5th ed., Taylor & Francis Group, New York, NY, 2007.

[11] D. Noel, M. Ritou, and B. Furet, "Complete Analytical Expression of the Stiffness Matrix of Angular Contact Ball Bearings," *ASME J. Tribology*, vol 135, no. 10, 041101, 8 pp., 2013.

[12] K. H. Hunt and F. R. E. Crossley, "Coefficient of Restitution Interpreted as Damping in Vibroimpact," *ASME J. Appl. Mech*, vol. 42, no. 2, pp. 440-445, 1975.

[13] J. Cao, P. E. Allaire, T. Dimond, and S. Dousti, "Auxiliary Bearing System Optimization for AMB Supported Rotors Based On Rotor Drop Analysis – Part 1: Rotor Drop Analysis Method," *Proceedings of ASME Turbo Expo*, GT2016-56323, Seoul, South Korea, 2016.

[14] J. Cao, P. E. Allaire, T. Dimond, and S. Dousti, "Auxiliary Bearing System Optimization for AMB Supported Rotors Based On Rotor Drop Analysis – Part 2: Optimization for Example Vertical and Horizontal Machines," *Proceedings of ASME Turbo Expo*, GT2016-56324, Seoul, South Korea, 2016.

[15] J. Cao, T. Dimond, P. E. Allaire, J. J. Rensberg, and C. Klatt, "Rotor Drop Analysis and Auxiliary Bearing System Optimization for AMB Supported Rotor – Part I:Analysis Method," *Proceedings of the Fifteenth International Symposium on Magnetic Bearings*, Kitkyushu, Japan, 2016.

[16] J. Cao, T. Dimond, P. E. Allaire, J. J. Rensberg, and C. Klatt, "Rotor Drop Analysis and Auxiliary Bearing System Optimization for AMB Supported Rotor – Part II: Experiment and Optimization," *Proceedings of the Fifteenth International Symposium on Magnetic Bearings*, Kitkyushu, Japan, 2016.